Distribution Agreement

In presenting this thesis as a partial fulfillment of the requirements for a degree from Emory University, I hereby grant to Emory University and its agents the non-exclusive license to archive, make accessible, and display my thesis in whole or in part in all forms of media, now or hereafter now, including display on the World Wide Web. I understand that I may select some access restrictions as part of the online submission of this thesis. I retain all ownership rights to the copyright of the thesis. I also retain the right to use in future works (such as articles or books) all or part of this thesis.

Claire Qu April 1, 2024

Gasdermin A is activated by *Staphylococcus aureus* cysteine protease Staphopain A

by

Claire Qu

Christopher LaRock, Ph.D

Adviser

Department of Biology

Christopher LaRock, Ph.D

Adviser

Nic Vega, Ph.D

Committee Member

Lindsey Seldin, Ph.D

Committee Member

2024

Gasdermin A is activated by *Staphylococcus aureus* cysteine protease Staphopain A

By

Claire Qu

Christopher LaRock, Ph.D

Adviser

An abstract of
a thesis submitted to the Faculty of Emory College of Arts and Sciences
of Emory University in partial fulfillment
of the requirements of the degree of
Bachelor of Science with Honors

Department of Biology

2024

Abstract

Gasdermin A is activated by *Staphylococcus aureus* cysteine protease Staphopain A

By Claire Qu

Methicillin-resistant *Staphylococcus aureus* (MRSA), is a gram-positive bacterium that is part of the human nasal microbiota. It is also a common opportunistic pathogen associated with community and hospital-acquired infections which causes sepsis and death. MRSA releases a cysteine protease, staphopain A (ScpA) during host epithelial cell cytoplasm invasion that induces cell death by an unknown mechanism. Pyroptosis, or inflammatory cell death, is important for initial host cell survival and signaling during infection. Gasdermin A (GSDMA), a pyroptosis-inducing protein expressed in human mucosa and epithelial cells is only known to be activated by the cysteine protease SpeB from Group A *Streptococcus* (GAS). Since GAS and MRSA clinical manifestations are similar, and SpeB and ScpA are both secreted cysteine proteases, it was hypothesized that GSDMA is activated by ScpA and that this is responsible for the cell death of keratinocytes observed during MRSA invasion. The data from biochemical assays and *in vivo* murine studies showed that ScpA affected the GSDMA pathway and induced other inflammatory signals. ScpA was able to cleave GSDMA *in vitro* to a form consistent with its activation. Murine GSDMA knockout and wild type C57Bl/ 6 mice, infected intradermally with wild type (WT) and ScpA deletion mutant (ΔScpA) MRSA strains had similar CFU burden and lesion sizes, but differences in redness and swelling consistent with a role for ScpA and GSDMA in the inflammatory response to infection. Pro-inflammatory cytokines like IL-1β were induced at higher rates with the WT MRSA injection rather than the ΔScpA MRSA injection. The cytokine concentration difference was more pronounced in GSDMA-KO mice than the WT mice. Overall, it was shown that ScpA plays a role for inflammation in MRSA infection and can cleave GSDMA. ScpA is not required for MRSA virulence as SpeB is required for GAS virulence. This data will inform further studies on ScpA and GSDMA interaction with keratinocytes using cell culture models, biochemical assays, and additional murine models of infection.

Gasdermin A is activated by *Staphylococcus aureus* cysteine protease Staphopain A

By

Claire Qu

Christopher LaRock, Ph.D

Adviser

A thesis submitted to the Faculty of Emory College of Arts and Sciences
of Emory University in partial fulfillment
of the requirements of the degree of
Bachelor of Science with Honors

Department of Biology

2024

Acknowledgements

I would like to thank Dr. Chris LaRock for mentoring me the past three years and showing me how to be a better scientist, academic, and person in general. I would also like to thank Dr. Doris LaRock for guiding me through this project and teaching me skills that I will carry with me far after graduation. I am grateful for the other members of the LaRock Lab, Ananya Dash, and Stephanie Guerra, as well as past lab members Dr. Anders Johnson and Emily Heathcote for their continuous support during my time in the lab. Additionally, I thank the McGavin lab for graciously providing the *S. aureus* strains for this project. Lastly, I would like to thank Dr. Nic Vega for advising me through the Biology B.S. degree the past two years and Dr. Lindsey Seldin for taking the time to serve on my thesis committee.

Table of Contents

Chapter 1: Introduction **8**

Chapter 2: ScpA activates hGSDMA and inflammation in vitro **12**

Figure 1. 12

Methods 13

Results 15

Figure 2. 15

Chapter 3: ScpA activates GSDMA and inflammation in vivo **15**

Figure 3. 16

Methods 18

Results 22

Figure 4. 22

Figure 5. 23

Figure 6. 24

Figure 7. 25

Figure 8. 27

Figure 9. 29

Chapter 4: Discussion and Conclusion **31**

Discussion 31

Future Directions and Conclusion 34

References **37**

Chapter 1: Introduction

Staphylococcus aureus is a gram-positive bacterium that infects a number of hosts. The name comes from the grape cluster-like morphology that is observed in *S. aureus* cells since Staphyle in Greek means "bunches of grapes". In humans, it is a major opportunistic pathogen and is associated with both community and hospital-acquired infections (Taylor and Unakal 2023). *S. aureus* is commonly colonized in the anterior nares as part of the normal microflora (Wertheim 2005). However, it can infect virtually every type of tissue in the human body and is connected to a broad range of clinical manifestations. It is a leading cause of sepsis, infective endocarditis, and pneumonia (Tong et al 2015). It is also a common cause of device-related, pleuropulmonary, osteoarticular, and skin and soft tissue infections (Tong et al 2015). In severe cases, *S. aureus* colonization may result in necrotizing fasciitis (NF) which is an aggressive and rapidly progressing superficial fascia infection with a high mortality rate (Sabat et al 2022). *S. aureus* can also live on the skin without overt infection, but still be associated with disease. One of the most common chronic inflammatory skin disorders, atopic dermatitis (AD), is associated with *S. aureus* colonization (Kim et al 2019). Patients with psoriasis, a chronic inflammatory skin condition that affects around 60 million people worldwide, also have increased *S. aureus* skin colonization, and *S. aureus*-induced inflammation is correlated with psoriasis pathogenesis (Raharja et al 2021) (Totté et al 2016).

In the past few decades, there has been a sharp increase in the prevalence of antibiotic-resistant strains like methicillin-resistant *Staphylococcus aureus* (MRSA) and vancomycin-resistant *Staphylococcus aureus* (VRSA), making it more complicated to treat *S. aureus* infections (Wertheim 2005). Antibiotic-resistant *S. aureus* infections are largely nosocomial; however, some strains, like the USA300 MRSA strain, are associated with community epidemics

(Wertheim 2005). Along with antibiotic resistance, these strains are particularly dangerous pathogens due to their destructive virulence factors (Watkins 2012). In the late 1990s and early 2000s, incidence rates of MRSA increased alarmingly throughout North America and Europe but due to improvements in infection control procedures, has since steadily decreased since 2005 (Tong et al 2015). However, there is still no vaccine against *S. aureus* (Clegg et al 2021).

To further develop therapies and infection control procedures, the complex pathophysiological interactions between *S. aureus* and the host must be better understood. *S. aureus* is known to make a range of virulence and immune invasion factors to alter the human immune response (Howden et al 2023). It also is known to invade non-phagocytic mammalian cells like keratinocytes as well as survive internalization of phagocytes like macrophages (Fraunholz and Sinha 2012). *S. aureus* can survive phagolysosome internalization by resisting host cell antimicrobial attack (Flannagan et al 2018). Invasion into the cytosol of non-phagocytic cells can also happen and is facilitated by numerous bacterial cell wall anchored proteins (Foster et al 2014). The bacteria can then kill the host cell from within and begin a new cycle of infection (Stelzner et al 2021). This internalization and release cycle leads to the persistence of the infection and the destruction of host tissue.

Several virulence factors are responsible for aiding host cell destruction (Stelzner 2021). Staphopains are highly conserved extracellular cysteine protease *S. aureus* virulence factors (Stelzner et al 2021). Staphopain A (ScpA) has a broad substrate specificity and is known to degrade elastin fibers and human complement proteins (Jusko et al 2014). ScpA is coded on the *scpAB* operon together with staphostatin B, which is responsible for 1:1 inhibition of ScpA proteolytic functions to protect from unnecessary protein degradation before the protease is secreted (Nickerson et al 2009). ScpA was identified to also induce cell death after host epithelial

cell cytoplasm invasion (Stelzner et al 2021). The mechanism by which cell death is induced is, however, unknown.

Mammalian hosts have endogenous mechanisms to detect and protect against bacterial invasion into the cytosol. When a host cell detects an intracellular pathogen like bacteria, the innate immune system is activated and assembles a supramolecule called the inflammasome (Deng et al 2022). The inflammasome mediates caspase-1 protease regulation which cleaves pro-inflammatory signaling cytokines interleukin-1β (IL-1β) and interleukin-18 (IL-18) into their biologically relevant forms (Kelley et al 2019). Once activated, cytokine IL-1β induces the expression of genes responsible for fever, pain, vasodilation, hypotension, and immune cell recruitment (Kelley et al 2019). IL-18 mediates initiation of adaptive immune responses and induction of the critical signaling cytokine interferon-gamma (IFN-γ) (Kelley et al 2019).

Gasdermins (GSDMs) are a family of five pore-forming proteins labeled A through E that are continuously expressed in the cytosol of a variety of mammalian host cells (Broz et al 2019). Along with cytokines, Caspase-1 is also shown to cleave gasdermin D in gut, liver, and lymph tissues (Orning et al 2019). Once cleaved, they are responsible for the lytic pro-inflammatory cell death program called pyroptosis (Broz et al 2019). It is thought that GSDMs induce pyroptosis as an immune mechanism to kill infected host cells and amplify inflammatory responses by releasing active IL-1β /IL-18, caspases, and other cytokines and inflammatory mediators (Liu et al 2021). Gasdermin proteins have an N-terminal cytotoxic domain and a C-terminal repressor domain connected by a linker (Broz et al 2019). Once cleaved, the N-terminal product is released which oligomerizes and punctures a hole in the cell membrane. This causes GSDM pore formation at membrane sites in the cell, initiating downstream inflammatory cascades and danger signals by releasing cytokines which induce inflammatory gene expression

in other cells within its vicinity (Liu et al 2021). Once the contents are released through the pores, the cell itself dies which leads to pathogen colony niche destruction (Orning et al 2019).

Gasdermin A (GSDMA) expressed in human mucosa, epithelial, and sentinel immune cells, has no known endogenous activation protein (Deng et al 2022). However, an extracellular cysteine protease, SpeB, from *Streptococcus pyogenes* (Group A *Streptococcus*, GAS) has been previously shown to uniquely activate GSDMA by cleaving the N-terminal product (Deng et al 2022) (LaRock et al 2022). *S. pyogenes* clinical manifestations are similar to that of *S. aureus* and infect the same cell types like keratinocytes. SpeB and ScpA are both virulence factors with cysteine protease functionality and have been shown to induce cell death after intracellular pathogen invasion. Conservation of GSDMA in the human genome indicates it could be important for detecting additional pathogens, and if so, *S. aureus* is one candidate.

In this thesis, I will examine the mechanism of ScpA-induced host epithelial cell death. The hypothesis is that ScpA, like SpeB, cleaves GSDMA specifically to initiate inflammatory cell death through pyroptosis. ScpA and SpeB have similar active sites and are both virulence factors known to cleave host proteins. Through biochemical assays and a necrotizing fasciitis mouse model of infection, I showed that the *S. aureus* secreted protease ScpA can indeed affect the GSDMA pathway as well as induce other inflammatory signals.

Chapter 2: ScpA activates hGSDMA and inflammation *in vitro*

It is hypothesized that since SpeB can cleave human GSDMA (hGSMDA), then ScpA can perhaps also cleave GSDMA at the same site to form a GSDMA pore (**Figure 1**). To examine whether GSDMA is indeed activated by ScpA with a similar mechanism to SpeB, purified ScpA and GSDMA proteins were incubated at physiological temperature and checked for cleavage products. If ScpA cleaves GSDMA at the same site at SpeB, the cleavage products should migrate similarly by SDS-PAGE.

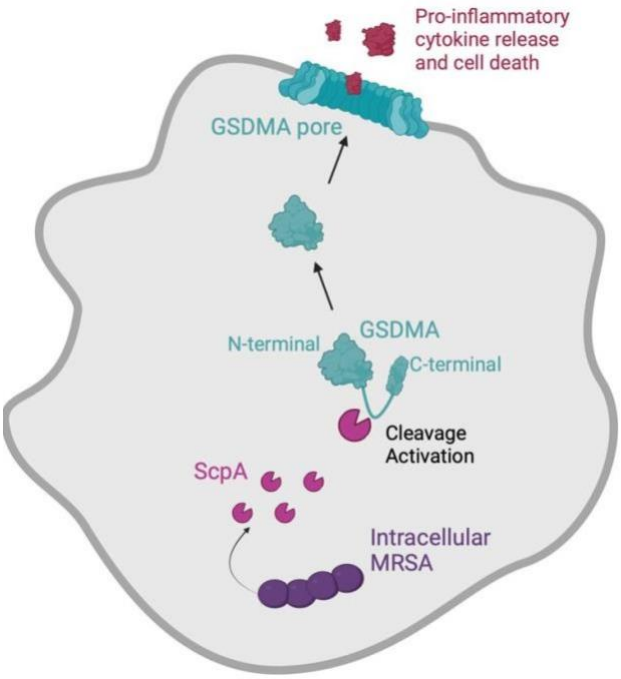

Figure 1. The schema shows the proposed mechanism of ScpA-activated, GSMDA-mediated pyroptosis. ScpA is released by intracellular MRSA which along with other functions, cleaves off the GSDMA suppressor C-terminal to induce the GSDMA N-terminal pore formation which causes pro-inflammatory cytokine release and cell death.

Methods

Protein Purification

The biochemical aspect of the project started with purifying ScpA and hGSDMA. ScpA was expressed and purified by expressing the protein in *S.aureus* RN6390 harboring pRscpAB plasmid (Ngai 2011). The cells were grown for 6 hours in Invitrogen Terrific Broth and separated by centrifugation (Ngai 2011). To chelate metals, 1 mM EDTA was added to the supernatant and the proteins were precipitated by the addition of 80% saturation of ammonium sulphate (Nickerson 2009). The pellet was dissolved and dialyzed into 20 mM sodium phosphate at pH 7.4. The protein was then filtered through a 0.20 μM filter before running a HiTrap SP HP ion exchange column (Amersham Biosciences). The proteins and ScpA were eluted in 2 mL fractions at a flow rate of 2 mL/min through a linear NaCl gradient up to 1.0 M in 50 mM sodium phosphate. The column fractions were visualized using sodium dodecyl-sulfate polyacrylamide gel electrophoresis (SDS-PAGE). Full-length human GSDMA was cloned from pUNO1-hGSDMA into pET-SUMO kanamycin cassette with a cleavable His-SUMO tag using the Polymerase Incomplete Primer Extension (PIPE) cloning technique (LaRock 2022). Protein expression of hGSMDA in *E. coli* BL21 (DE3) was then induced at 18C overnight with 0.2 mM isopropyl-β-d-thiogalactopyranoside (IPTG) until OD_{600} reaches to 0.8. Cells were collected and resuspended in lysis buffer (20 mM Tris HCl, pH 8.0, 150 mM NaCl, 1 mM DTT). Lysates were homogenized through ultrasonification. His6-SUMO-hGSDMA was purified using affinity chromatography with HisPur Nickel Resin. The column fractions were visualized using sodium dodecyl-sulfate polyacrylamide gel electrophoresis (SDS-PAGE).

Cleavage Assays

Once purified, the activity of ScpA on hGSDMA was checked. GSDMA was incubated with ScpA at various concentrations and time periods to identify the cleavage conditions. Initially, ~6 μm of purified recombinant GSDMA (300 ng/μL) and ScpA at 20 ng/μL were incubated in cleavage buffer (phosphate-buffered saline (PBS), 2 mM DTT, 2 mM EDTA), then separated by SDS-PAGE and visualized using AcquaStain (Bulldog Bio) staining of proteins. For kinetics of cleavage, ~6 μm of purified recombinant GSDMA (300 ng/μL) was incubated at 37°C with ~3 μm of ScpA (with the optimal concentration). Aliquots of the sample were taken out at 0 minutes, 15 minutes, 30 minutes, 1 hour, 2 hour, and 4 hours. The products were separated on a sodium dodecyl-sulfate polyacrylamide gel electrophoresis (SDS-PAGE) protein gel and visualized using AcquaStain (Bulldog Bio) staining of proteins.

Results

Protein Purification and Cleavage Assay

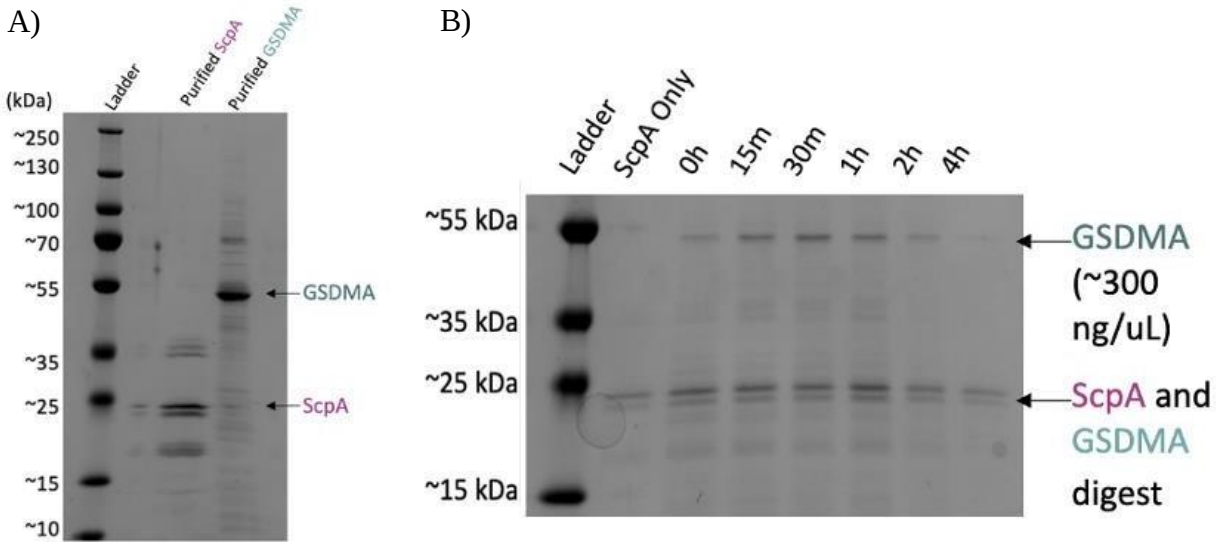

Figure 2. **A)** SDS-PAGE protein gels verifying the presence of purified human GSDMA and ScpA. **B)** The time course cleavage assay was visualized through an SDS-PAGE protein gel. The cleavage of recombinant human GSDMA was then verified.

Inactivated hGSDMA has a molecular weight of 49.4 kDa. ScpA has a molecular weight of 21 kDa. The purified human GSDMA and MRSA ScpA tested were not completely clean (**Figure 2A**). In PBS and physiological temperatures at the concentrations tested, hGSDMA cleavage seems to happen around the one-hour time point, evidence by the loss of intensity of the ~50 kDa band of hGSDMA (**Figure 2B**). Along with the linker, there may be additional cleavage of the C- and N-terminal fragments by ScpA which prevents their accumulation under these conditions (**Figure 2B**). Additionally, the N- and C-terminals of GSDMA have similar molecular weights as ScpA at around 28 kDa and 24 kDa respectively.

Chapter 3: ScpA activates GSDMA and inflammation *in vivo*

To test if GSDMA is activated by ScpA *in vivo*, murine models were used. Like humans, mice express mGSDMA which is similar to hGSDMA in the skin and upper gastrointestinal tract. Unlike humans, mice express three tandem alleles (mGSDMA 1-3) on chromosome 11 which appear in different concentration in each tissue: mGSDMA1 is expressed in the skin and the stomach, mGSDMA2 is highest in the stomach, and mGSDMA3 is highest in the skin (LaRock et al 2022) (**Figure 3**). GAS cysteine protease SpeB was shown to cleave all three mGSDMAs with possible functional redundancy. Thus, to phenocopy the single human GSDMA gene, mGSDMA123-triple-knockout mice were used.

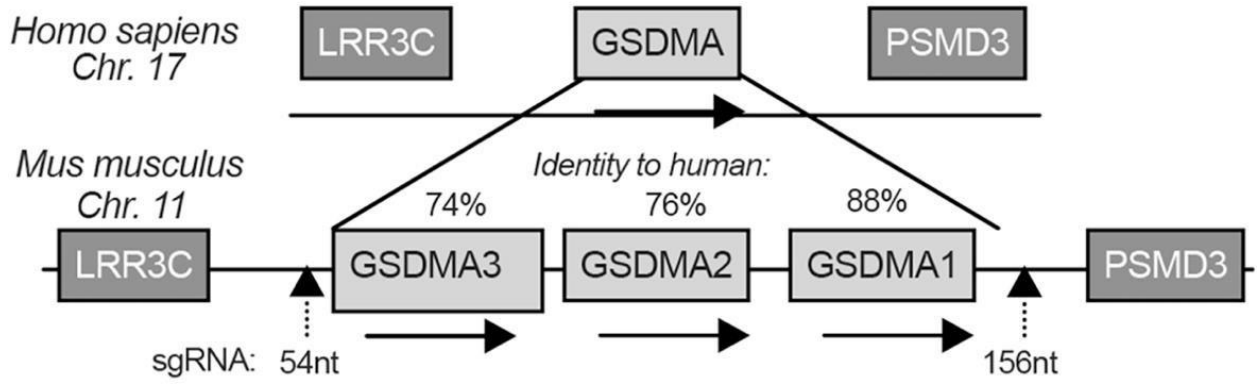

Figure 3. GSDMA gene arrangement in mice along with the human homolog. GSDMA knock out mice were bred for experimentation using CRISPR. The CRISPR site is indicated (LaRock et al 2022).

The murine model of infection was used where a necrotizing fasciitis lesion is induced between the epidermis and dermis by an intradermal injection of either wild type MRSA (WT MRSA) and ScpA deletion mutant MRSA (ΔScpA MRSA) strains into wild type C57B1/6 or mGSDMA1,2,3-KO mice. Such lesions are observed clinically in human skin infections like necrotizing fasciitis (Sabat 2022). Mice skin lesions were then dissected and analyzed through

visual measurements, pathogenic bacteria colony forming units (CFU), and inflammation-associated cytokine concentrations. Visual measurements were taken to compare quantitative visual differences of lesions between conditions. MRSA CFUs were measured to quantify bacterial load of the skin infection between conditions. Inflammation-associated cytokine concentrations were measured to identify the inflammatory levels between conditions.

Methods

Strain Preparation

The *S. aureus* strains were graciously given by the McGavin lab at Western University. Pandemic *S. aureus* strain WBG10049, a strain that produces ScpA, was used as the wild type (WT) MRSA strain and has been described previously (Nickerson et al 2010). The ScpA knock-out (ΔScpA) MRSA strain was created by replacing the *scpAB* operon with an aminoglycoside-resistance cassette in WBG10049 as previously described (Ngai 2011). The strains were routinely propagated at 37°C in Tryptic Soy Broth (TSB; Difco) and washed two times with PBS before diluting to $1x10^9$ colony forming units per mL (CFU/mL).

Mice Breeding and Knockout Mice Generation

Triple mouse GSDMA (mGSDMA) knockout C57B1/6 mice are previously described, generated by using CRISPR/Cas9 to eliminate the coding sequence of all three GSDMA genes and did not include any overlapping genes on either DNA strand (LaRock 2022). Genotyping was performed to verify knockout mice using ear clip samples in lysis reagent (25mM NaOH, 0.2mM EDTA). To extract the DNA, the sample was heated at 95°C for 1 hour and then cooled to room temperature before 75 μL of 40mM Tris pH 5 was added. A PCR reaction was completed using two primers:

GSDMA-F (GCCTGAGGTGAGGCACTTCTAACAG)

GSDMA-R (GCACGAGGCACACAAGTGGTGCAC).

The PCR sample (5μL 5x GoTaq Flexi buffer, 2μL 25mM $MgCl_2$, 0.5μL 10mM dNTPs, 0.125μL GoTaq Hot Start Polymerase, 2.5μL Template DNA, 13.9 μL Water, 1μL 5μM F/R primer mix) was incubated at 95°C for 3 minutes. Then repeating, 95°C for 15 seconds

(denaturing), 54°C for 15 seconds (annealing), 72°C for 1 minute (elongation), 34 times. The final elongation was set as 72°C for 5 minutes and the sample was held at 12°C. PCR samples were run on 2% agarose gel for visualization.

Intradermal Mice Infection

Six to twelve week old C57B1/6 WT and GSDMA KO (mGSDMA1,2,3-KO) mice of both sexes were first injected intradermally with 1 x 10^7 or 1x 10^9 100 μL of WBG10049. Each injection site was shaved, exfoliated, and disinfected with ethanol before inoculation. They were then housed in the standard ambient ABSL-2 environment (~20°C and ~50% humidity) under pathogen-free conditions with a 14 hour light/ 10 hour dark cycle. After 48 hours, the mice were euthanized by CO_2 asphyxiation and decapitation. The skin lesions were imaged for size analysis and color change observations. Skin lesion and spleen samples were then disinfected with ethanol and dissected from each experiment for CFU plating, Inflammatory Cytokine Array analysis, and histology analysis. Animal use and procedures were approved by the Emory Institutional Care and Use Committee.

Skin Lesion Size Analysis

The analysis of skin lesion size was conducted utilizing FIJI software. Photographic documentation of the skin lesions included the inclusion of a ruler for scale reference. The measurement of the lesion surface area was conducted to assess the extent of horizontal tissue damage expansion.

Color Quantification

The analysis of inflamed uninfected skin (IUS) redness around the lesion was conducted utilizing FIJI software. Photographic documentations of the skin lesions were split into CIEL*A*B* color space. The a* image was then selected. The a* image applies the a* value, color from green (-60) to red (+60), to each pixel of the image. The mean value of a* of a selected area at the IUS was measured and compared to a representative a* measured at an uninflamed uninfected skin area (UUS) serving as a control site for background skin redness. Thus, Δa^* is the difference between the IUS and the UUS a* values. Adapted from Logger, J. G. M., E. M. G. J. de Jong, R. J. B. Driessen, and P.E. J. van Erp (2020).

Histology

Histology was performed on the mice skin samples to visualize tissue damage and immune cell accumulation at the subcutaneous injection site. The skin lesion samples were first fixed in 4% paraformaldehyde, paraffinized, and sectioned at a width of 5 μm and then sent to the Cancer Tissue and Pathology Shared Resource of Winship Cancer Institute of Emory University for slide preparation. The sample was then stained with hematoxylin and eosin (H&E) to identify types of cells and tissue in the sample. Nuclei will be observed to identify neutrophil accumulation and epithelium damage.

Colony Forming Units (CFU) Analysis

Mice skin samples were homogenized in 180 μL of PBS with a bead mill and subsequently prepared for CFU plating to quantify the bacterial load within the lesions. Following homogenization, the samples were appropriately diluted and plated on HARDYCHROM MRSA

(Hardy Diagnostics) plates and incubated at 37°C overnight. The resultant bacterial colonies were then enumerated as CFU/mL by multiplying the number of colonies by the total dilution factor and dividing the result by the volume of culture plated in milliliters. correlated with the respective skin lesion sizes.

Inflammatory Cytokine Concentrations

Cytokine arrays were conducted to determine cytokine levels in the supernatant of the homogenized murine lesion tissue. The V-PLEX proinflammatory Panel 1 Mouse Kit was used and measured the expression of the cytokines IL-15, IL-33, MCP-1, IL-17A, IL-9, MIP-1α, IL-27p28, IP-10, MIP-2, IFN-γ, IL-10, IL-12p70, IL-1β, IL-2, IL-4, IL-5, IL-6, TNF- α, KC/GRO. The total protein content from the supernatants was quantified by using Pierce Coomassie Plus (Bradford) Assay Reagent (Thermo Fisher). The total protein content was then normalized to 40µg per sample. Quantification and analysis were done by the Emory Multiplexed Immunoassay Core (EMIC) with a QuickPlex SQ120 (Meso Scale Discovery).

Statistics

Graphpad Prism 9 was used to evaluate statistical significance. All quantitative data were analyzed used ANOVA multiple comparisons with Bonferroni correction (n=7,8,7,8). *P*-values < 0.05 were considered significant.

Results

Skin Lesion Analysis and Color Quantification (CQ)

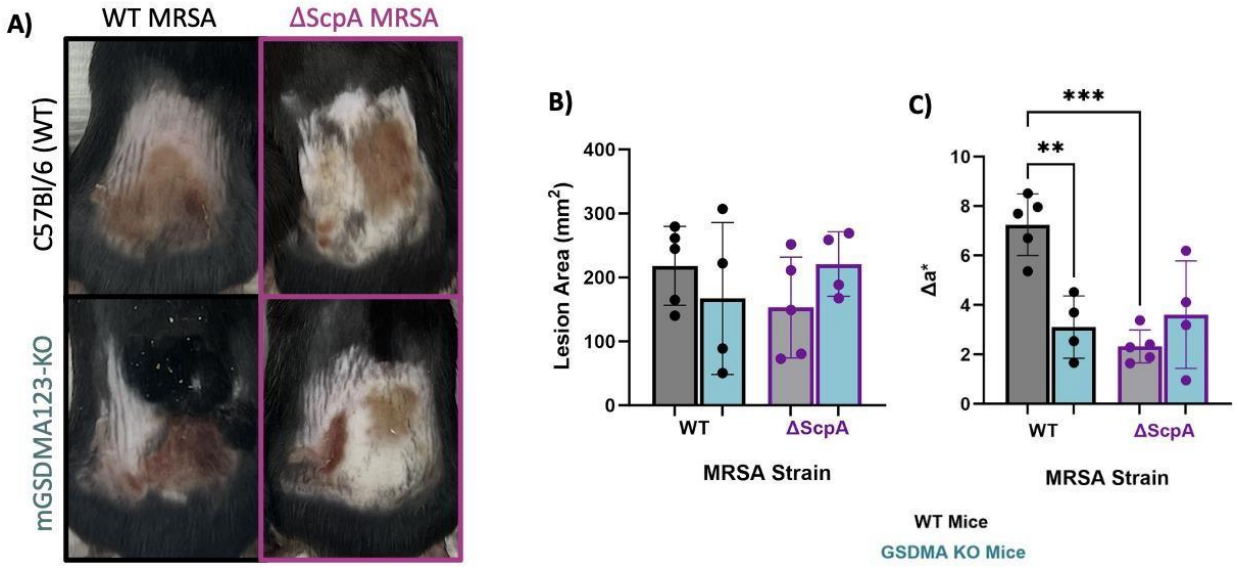

Figure 4. **A)** Representative subcutaneous skin lesions of WT mice and mGSDMA123-KO mice 48 hours after intradermal injection of 10^7 CFU of WT MRSA or ΔScpA MRSA. **B)** Measured lesion areas of mice 48 hours after intradermal injection. P values were calculated using ANOVA multiple comparisons with Bonferroni correction (n=5,4,5,4). **C)** Non-lesion skin areas were measured for changes in color to identify skin inflammation. The a* value indicates the mean color value from green (-60) to red (+60) of the selected area. The Δa* value is the normalized a* value difference between inflamed uninfected skin area and uninflamed infected skin area of the same mouse. P values were calculated using ANOVA multiple comparisons with Bonferroni correction (n=5,4,5,4).

The absence of ScpA or GSDMA have no obvious visual effect on the appearance of MRSA infection lesions. The lesion appearances were variable among biological replicates in all four conditions (**Figure 4A**). Neither ScpA nor GSDMA had a significant effect on MRSA lesion size, possibly in part due to the biological replicates in all four conditions varied greatly in lesion size (**Figure 5B**). WT mice infected with WT MRSA had the highest Δa* value and thus

had the higher red intensities at inflamed uninfected skin (IUS) areas (**Figure 5C**). The absence of ScpA decreases red intensity of IUS areas in WT mice (**Figure 5C**). Since redness is associated with inflammation, WT MRSA infected WT mice, therefore, were associated with more inflammation than the other attenuated groups (**Figure 5C**).

Colony Forming Units Analysis

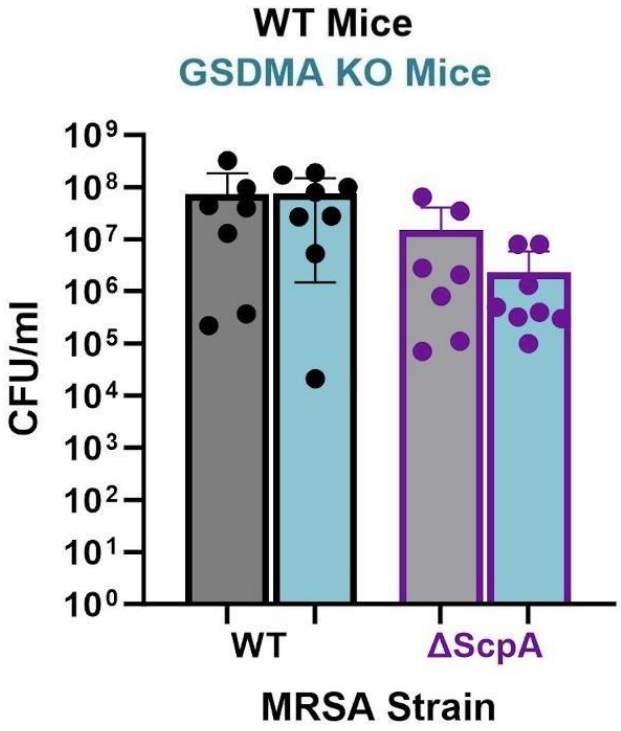

Figure 5. Colony forming units of MRSA from dissected skin lesions of WT Mice and mGSDMA1,2,3-KO mice 48 hours after infection with 10^9 CFU WT MRSA and ΔScpA MRSA. P values were calculated using ANOVA multiple comparisons with Bonferroni correction (n=7,8,7,8).

MRSA bacterial burden in mice lesions were variable among biological replicates in all four conditions (**Figure 6**). The mGSDMA1,2,3-KO mice carried a trending lower bacterial load when infected with ΔScpA MRSA compared to WT MRSA (**Figure 6**).

Skin Lesion Histology

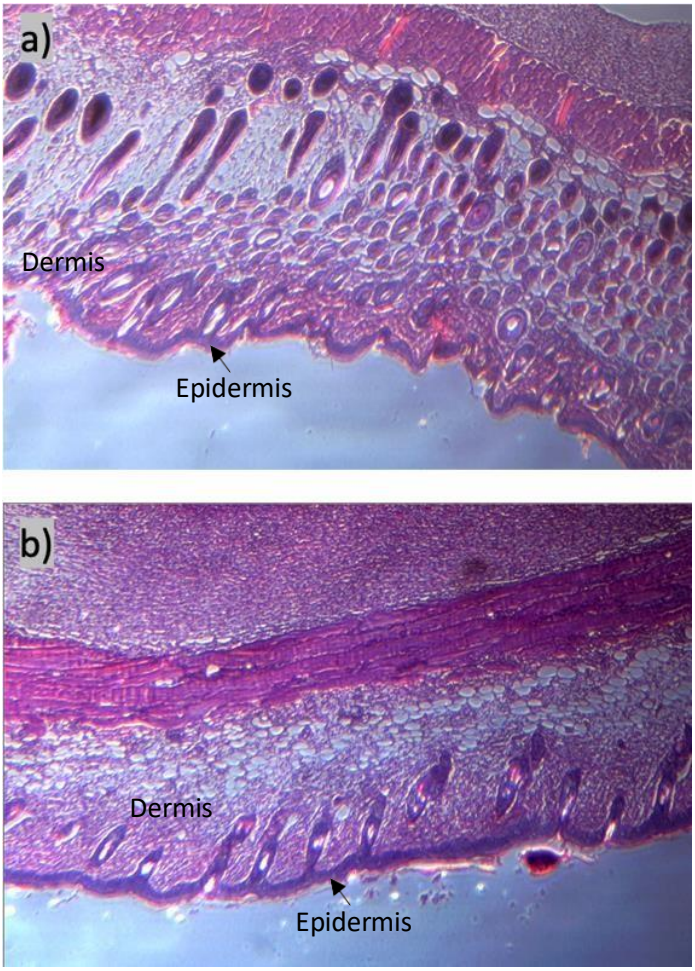

Figure 6. **a)** Images of hematoxylin- and eosin-stained (H&E) histological sections of WT MRSA infected WT mice skin lesions 48 hours after bacterial injection taken at 40x magnification.
b) ΔScpA MRSA infected WT mice skin lesion H&E histology images 48 hours after bacterial injection taken at 40x magnification.

H&E histology images were taken of WT mice lesions only (**Figure 6**). From microscopy examination, the epidermis of the WT MRSA infected skin lesions was observed to have poor organization of dermis layers and abundant inflammatory infiltrate (**Figures 6a**). The epidermis of the ΔScpA MRSA infected skin lesions were observed to have better organization of dermis layers and less abundant inflammatory infiltrate (**Figures 6b**).

Cytokine Array Analysis

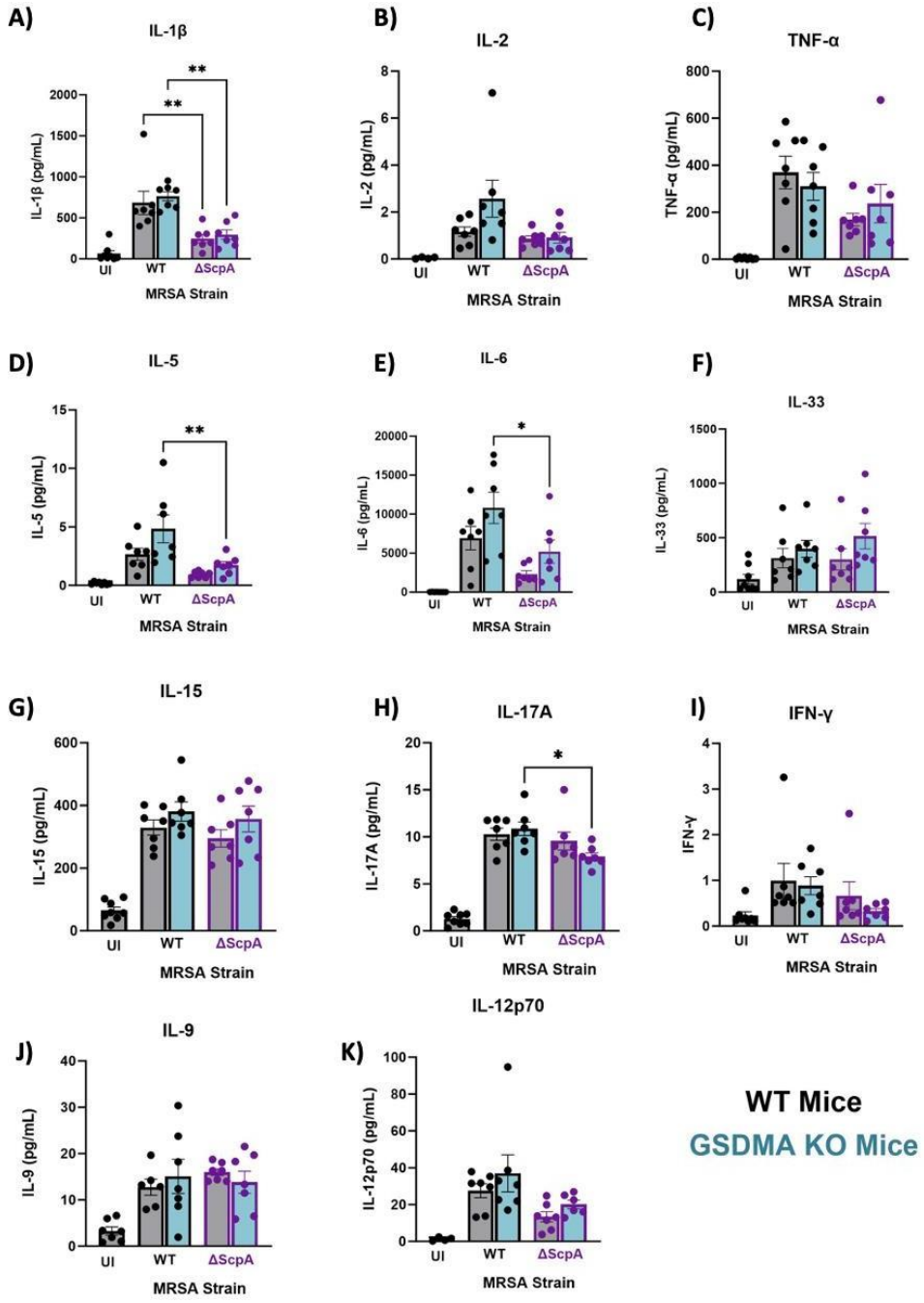

Figure 7. Concentration measurements of pro-inflammatory cytokine expression from skin lesions. Skin lesions were dissected from WT and mGSDMA1,2,3-KO mice 48 hours after infection with 10^9 CFU WT MRSA and ΔScpA MRSA. Uninfected (UI) WT mice skin was also dissected and analyzed as a negative control. P values were calculated using ANOVA multiple comparisons with Bonferroni correction (n=7,7,7,7).

Generally, the pro-inflammatory cytokines trended towards higher rates of induction with the WT MRSA rather than the ΔScpA MRSA injections (**Figure 7**). IL-1β expression in WT MRSA-infected mGSDMA1,2,3-KO mice skin lesions is significantly higher than expression in ΔScpA MRSA infected KO mice (**Figure 7A**). A similar trend is seen in WT mice (**Figure 7A**). IL-2 concentrations between conditions although were not statistically significant, shared a similar trend in only mGSDMA1,2,3-KO mice lesions to IL-1β where WT MRSA injections induced higher IL-2 expression than ΔScpA MRSA infection (**Figure 7B**). IL-5 expression in WT MRSA infected KO mice skin lesions is significantly higher than expression in ΔScpA MRSA infected KO mice (**Figure 7D**). IL-6 expression in WT MRSA infected KO mice skin lesions is significantly higher than expression in ΔScpA MRSA infected KO mice (**Figure 7E**). TNF-α, IL-33, IL-15, IFN-γ, IL-9, and IL12p70 did not seem to have any significant differences in concentrations between all four conditions (**Figures 7C, 7F, 7G, 7I, 7J, 7K**). IL-17A expression in WT MRSA infected mGSDMA1,2,3-KO mice skin lesions only is significantly higher than expression in ΔScpA MRSA infected KO mice (**Figure 7H**).

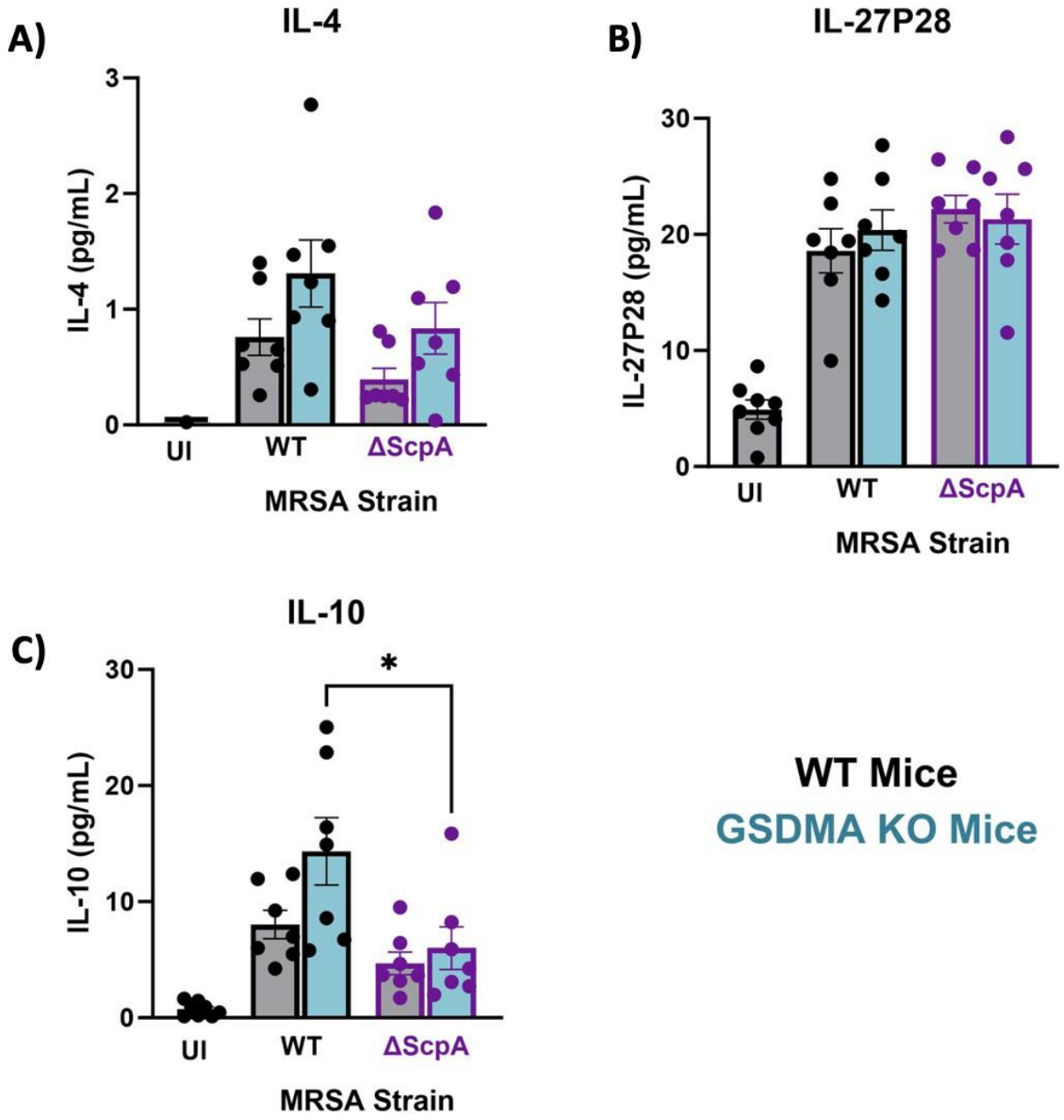

Figure 8. Concentration measurements of anti-inflammatory cytokine expression from skin lesions. Skin lesions were dissected from WT and mGSDMA1,2,3-KO mice 48 hours after infection with 10^9 CFU WT MRSA and ΔScpA MRSA. Uninfected (UI) WT mice skin was also dissected and analyzed as a negative control. P values were calculated using ANOVA multiple comparisons with Bonferroni correction (n=7,7,7,7).

Generally, the three anti-inflammatory cytokines trended towards higher levels of induction with the WT MRSA rather than the ΔScpA MRSA injections (**Figure 8**). IL-4 concentrations between conditions were not statistically significant due to high variability, however, there is a trend in both WT and mGSDMA1,2,3-KO mice where WT MRSA injections induced higher IL-4 expression than ΔScpA MRSA infection (**Figure 8A**). IL27p28 did not seem to have any significant differences in concentrations between conditions (**Figures 8B**). IL-10 expression in WT MRSA infected mGSDMA1,2,3-KO mice skin lesions is significantly higher than expression in ΔScpA MRSA infected KO mice (**Figure 8C**). A similar trend is seen in WT mice (**Figure 8C**).

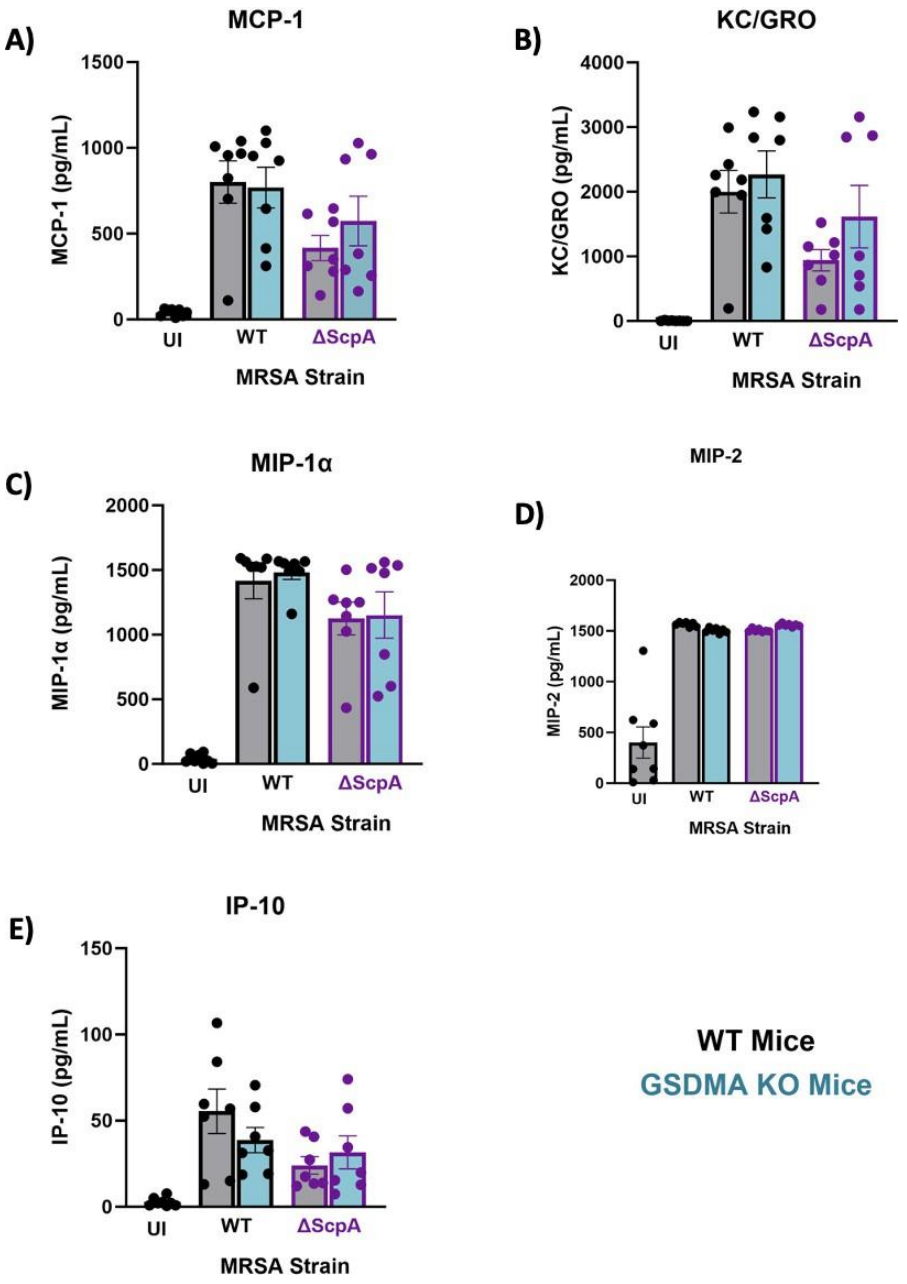

Figure 9. Concentration measurements of inflammatory chemokine expression from skin lesions. Skin lesions were dissected from WT and mGSDMA1,2,3-KO mice 48 hours after infection with 10^9 CFU WT MRSA and ΔScpA MRSA. Uninfected (UI) WT mice skin was also dissected and analyzed as a negative control. P values were calculated using ANOVA multiple comparisons with Bonferroni correction (n=7,7,7,7).

Inflammatory chemokine expression trended towards higher in the WT MRSA infections rather than the ΔScpA MRSA injections in WT mice (**Figure 9**). MCP-1, KC/GRO, MIP-1α, MIP-2, and IP-10 did not seem to have any significant differences in concentrations between conditions (**Figures 9A, 9B, 9C, 9D, 9E**).

Chapter 4: Discussion and Conclusion

Discussion

Pyroptosis pores are classically induced by the cleavage of GSDMD by caspase-1. Unlike GSDMD, GSDMA is selectively expressed in skin and gastrointestinal tissue and has no known endogenous activator. However, the *Streptococcus pyogenes* virulence protease, SpeB, was previously shown to cleave GSDMA during intracellular infections at the linker in positions 244-245 and 245-246 (LaRock et al 2022). SpeB subsequently activates GSDMA to induce inflammatory cell death which is important to host survival during microbial infection (Deng et al 2022). In GAS keratinocyte infections, the absence of GSDMA leads to more severe infections in mice like a higher number of colony forming units and lesion sizes of the infected site (Larock et al 2022). The *Staphylococcus aureus* and MRSA virulence factor, ScpA, is a broad specificity papain-like protease like SpeB. ScpA is known to induce host cell death in epithelial cells (Stelzner et al 2021). Additionally, since *S. aureus* is a part of the normal skin microbiota like GAS and GSDMA expressed in the skin, it was also thought that *S. aureus* may have developed interactions with GSDMA (Wertheim 2005). ScpA is important for MRSA to penetrate the layers of keratinocytes, the first barrier of immune defense. Thus, it was hypothesized that ScpA cleaves GSDMA in the same way as SpeB to initiate keratinocyte cell death and amplify inflammatory signaling through pyroptosis.

In Chapter 2, it was shown that purified hGSDMA can be cleaved by purified ScpA in PBS at physiological temperature at around one hour of incubation (**Figure 2**). Therefore, there is interaction between GSDMA and ScpA. However, it is unclear where the cleavage site is, as the cleavage products are quickly degraded. It is likely that the role ScpA plays in GSDMA activation is more complicated than a simple cleavage activation at a linker site. Additionally, a

less pure GSDMA purification was also shown to be more effectively cleaved by ScpA which may indicate that other protein interactions may be occurring.

In Chapter 3, murine models were used for studies i*n vivo* because previous studies have shown that the three mouse GSDMA alleles (mGSDMA1, 2, and 3) function similarly to hGSDMA and are expressed in the skin and upper gastrointestinal tract (**Figure 3**). The inbred C57Bl/6 mouse line was used because the mice are genetically identical (Bryant 2016). Unlike the GAS-infected mice, MRSA-infected mGSDMA1,2,3-KO mice developed similar lesion sizes to MRSA-infected WT mice (LaRock 2022) (**Figures 4A, 4B**). It is likely that the experiment is underpowered (n=5) and further experimentation with larger sample numbers is needed. The lesion area for all conditions is also larger than GAS-infected WT and mGSDMA1,2,3-KO mice even though the initial CFU of the MRSA injections is ten-fold smaller than the GAS injections (LaRock 2022). MRSA infections also lead to faster lesion spreading, possibly due to differences in clumping and cell adherence (Yoshida et al 1979). It also was observed that MRSA infections can penetrate the dermis more easily than strep infections. However, WT MRSA-infected WT mice had significantly higher red intensities in non-lesion skin than the other conditions where GSDMA or ScpA were knocked out (**Figure 4C**). It is possible that the severity of inflammation around the skin lesions is dependent on the presence of both GSDMA and ScpA. Further studies need to be conducted to verify this cause and mechanism. The skin lesion CFU data also found no significance in the bacterial load between the conditions post 48 hours of infection (**Figure 5**). There is a slightly higher bacteria burden in the ΔScpA MRSA-infected GSDMA-KO mice lesions, however, the data has been inconsistent. Further studies utilizing different methods must be conducted to ensure reliability. Thus, GSDMA detection of ScpA will lead to detection of intracellular MRSA and an increase in inflammation but not a significant decrease in bacterial

load, unlike SpeB. Histology showed that WT MRSA infected WT mice had more epidermis and dermis damage and inflammation than ΔScpA MRSA infected WT mice (**Figure 6**).

The cytokine array shows the expression of inflammation associated cytokines in the skin lesions. It was observed that since IL-1β had higher concentrations in WT MRSA infected skin lesions than ΔScpA MRSA infected skin lesions, ScpA is important for the activation of IL-1β (**Figure 7A**). It is thus hypothesized for future experimentation that like SpeB, ScpA can cleave and activate IL-1β. Proteolytic cleavage of IL-1β initiates the inflammasome complex and other pro-inflammatory pathways (Kaneko et al 2019). ScpA was also observed to be important for the activation of IL-5 and IL-6, other pro-inflammatory cytokines (**Figures 7D, 7E**). IL-5, like the other pro-inflammatory cytokines, induces pleiotropic activities including B cell, eosinophil, and basophil activation or proliferation (Takatsu 2011). IL-6 specifically activates and maintains inflammatory responses as well as antimicrobials and is known to monitor the inflammation levels in bacterial infections (Kany et al 2019). TNF-α, IFN-γ, and IL12p70 expression data also showed that, specifically in WT mice, ScpA is important for the activation of these cytokines (**Figures 7C, 7I, 7K**). TNF-α is known to be responsible for a diverse range of signaling events that lead to necrosis and apoptosis (Idriss and Naismith 2000). IL12p70 upregulates NK cell and helper T cell proliferation (Hamza et al 2010). IL-17A expression data also show that in mGSDMA1,2,3-KO mice, ScpA is important for cytokine activation (**Figures 7H**). IL-17A is known to also amplify other pro-inflammatory cytokines as well as activate eosinophils (Kline et al 2023). IL-10, an anti-inflammatory cytokine, was shown to be upregulated in mGSDMA1,2,3-KO mice and ScpA is also important for the expression of it in KO mice (**Figure 8C**). The pro-inflammatory chemokines concentrations analyzed did not significantly increase with mutation of ScpA or GSDMA (**Figure 9**).

Future Directions and Conclusion

In conclusion, in Chapter 2, it was shown that hGSDMA can be cleaved by ScpA *in vitro*. The cleavage site has not been identified as the protein seems to be degraded at multiple sites by ScpA. Further studies must be conducted to verify the cleavage sites and the interactions between hGSDMA and ScpA. Additionally, the GSDMA cleavage products are also similar in molecular weight as ScpA which renders interpreting the SDS-PAGE gel difficult. Thus, different experimentation methods like western blot or mass spectrometry will be conducted to definitively detect and characterize the cleavage products. Additionally, liposome assays will be conducted to see if the GSDMA pore is created and induced after GSDMA cleavage by ScpA. These lipids could potentially protect activated GSDMA from further degradation by ScpA, as would likely happen inside a cell. *In vitro* infection experiments with keratinocyte from WT and GSDMA knock out mice will also be conducted with ΔScpA MRSA infection to examine if the cleavage product leads to pyroptosis and cell death. Immunofluorescent microscopy images of keratinocyte permeabilization may also be conducted to identify if the GSDMA pores are forming in keratinocytes.

In Chapter 3, it was shown that in murine models, GSDMA and ScpA both have an effect in pro-inflammatory immune processes. WT MRSA infected WT mice had higher red intensities than ΔScpA MRSA infected WT mice although lesion size differences between all mice conditions were variable and not significant. Although the KO mice carried a higher bacterial load when infected with ΔScpA MRSA compared to WT MRSA, the bacterial burden between all four conditions were relatively uniform since all groups had high biological variability. Therefore, ScpA is not as required for MRSA virulence as SpeB is for GAS infections (LaRock 2022). The inconclusive results and high variability in the lesion size measurement and colony

forming unit analysis could be due to the severity of the infection. Likely, the intradermal injection of 10^9 CFU of MRSA and subsequent 48 hours of infection could lead to infections too severe to compare initial inflammatory signaling and pyroptosis pathways. Thus, the differences in initial immune activation may not be detectable. To verify this conclusion, the mouse model must be altered and optimized for future experimentation. A gentler topical application model rather than an intradermal injection model may be employed. Topical application may also be more relevant the clinical onset of MRSA skin infections since infections usually start on the skin surface rather than subcutaneously (Mills et al 2022). Moreover, GSDMA is highly expressed in corneocytes, keratinocytes which make up the outermost layer of human skin (Lachner et al 2017). The intradermal injection model may have interacted with mostly fibroblasts in the subcutaneous space which do not express GSDMA. The timing of the lesion dissection could also be decreased from 48 hours to 24 hours and a lower bacteria dose could be applied for a slower infection. A slower infection could lead to more conclusive results as the group differences would be more pronounced. Additional measurements could also be taken like measuring lesion skin thickness. Better quality histology pictures of skin lesions could also be prepared when using the topical application model because the lesions would be less severe. H&E histology pictures of mGSDMA1,2,3-KO mice can also be taken in the future in addition to a negative, healthy skin control image.

In Chapter 3, pro-inflammatory cytokines were shown to be induced at higher rates with the WT MRSA injection rather than the mutant MRSA injection. However, the presence of GSDMA does not seem to affect the cytokine expression rates in mice skin lesion cells. It was also shown specifically that IL-1β has higher expression and activation when ScpA is present. SpeB is known to cleave IL-1β (LaRock et al 2016). Thus, it can be hypothesized that ScpA may

also cleave IL-1β in a similar way to SpeB. Future experimentation regarding this mechanism can also be conducted by performing a cleavage assay with the two proteins.

Overall, it was found that there is interaction between GSDMA and ScpA and ScpA is important for infection inflammation. However, more studies need to be conducted to identify GSDMA cleavage areas, GSDMA pore activation, and keratinocyte cell death due to GSDMA pore activation.

References

Broz, P., P. Pelegrín, and F. Shao, 2020 The gasdermins, a protein family executing cell death and inflammation. Nat Rev Immunol 20: 143–157.

TAKATSU, K., 2011 Interleukin-5 and IL-5 receptor in health and diseases. Proc Jpn Acad Ser B Phys Biol Sci 87: 463–485.

Clegg, J., E. Soldaini, R. M. McLoughlin, S. Rittenhouse, F. Bagnoli *et al.*, 2021 Staphylococcus aureus Vaccine Research and Development: The Past, Present and Future, Including Novel Therapeutic Strategies. Frontiers in Immunology 12:.

Deng, W., Y. Bai, F. Deng, Y. Pan, S. Mei *et al.*, 2022 Streptococcal pyrogenic exotoxin B cleaves GSDMA and triggers pyroptosis. Nature 602: 496–502.

Flannagan, R. S., R. C. Kuiack, M. J. McGavin, and D. E. Heinrichs, 2018 Staphylococcus aureus Uses the GraXRS Regulatory System To Sense and Adapt to the Acidified Phagolysosome in Macrophages. mBio 9: e01143-18.

Fraunholz, M., and B. Sinha, 2012 Intracellular staphylococcus aureus: Live-in and let die. Frontiers in Cellular and Infection Microbiology 2:.

Fry, L., and B. S. Baker, 2007 Triggering psoriasis: the role of infections and medications. Clinics in Dermatology 25: 606–615.

Hamza, T., J. B. Barnett, and B. Li, 2010 Interleukin 12 a Key Immunoregulatory Cytokine in Infection Applications. Int J Mol Sci 11: 789–806.

Howden, B. P., S. G. Giulieri, T. Wong Fok Lung, S. L. Baines, L. K. Sharkey *et al.*, 2023 Staphylococcus aureus host interactions and adaptation. Nat Rev Microbiol 21: 380–395.

Idriss, H. T., and J. H. Naismith, 2000 TNF alpha and the TNF receptor superfamily: structure-function relationship(s). Microsc Res Tech 50: 184–195.

Ikuta, K. S., L. R. Swetschinski, G. R. Aguilar, F. Sharara, T. Mestrovic *et al.*, 2022 Global mortality associated with 33 bacterial pathogens in 2019: a systematic analysis for the Global Burden of Disease Study 2019. The Lancet 400: 2221–2248.

Jusko, M., J. Potempa, T. Kantyka, E. Bielecka, H. K. Miller *et al.*, 2013 Staphylococcal Proteases Aid in Evasion of the Human Complement System. Journal of Innate Immunity 6: 31–46.

Kaneko, N., M. Kurata, T. Yamamoto, S. Morikawa, and J. Masumoto, 2019 The role of interleukin-1 in general pathology. Inflammation and Regeneration 39: 12.

Kany, S., J. T. Vollrath, and B. Relja, 2019 Cytokines in Inflammatory Disease. Int J Mol Sci 20: 6008.

Kelley, N., D. Jeltema, Y. Duan, and Y. He, 2019 The NLRP3 Inflammasome: An Overview of Mechanisms of Activation and Regulation. Int J Mol Sci 20: 3328.

Kim, J., B. E. Kim, K. Ahn, and D. Y. M. Leung, 2019 Interactions Between Atopic Dermatitis and Staphylococcus aureus Infection: Clinical Implications. Allergy Asthma Immunol Res 11: 593–603.

Kline, S. N., N. A. Orlando, A. J. Lee, M.-J. Wu, J. Zhang *et al.*, 2024 Staphylococcus aureus proteases trigger eosinophil-mediated skin inflammation. Proceedings of the National Academy of Sciences 121: e2309243121.

Ngai, W., 2011 Investigation of the *in vivo* function of Staphlopain A cysteine protease in *Staphylococcus aureus* infections.

Lachner, J., V. Mlitz, E. Tschachler, and L. Eckhart, 2017 Epidermal cornification is preceded by the expression of a keratinocyte-specific set of pyroptosis-related genes. Sci Rep 7: 17446.

LaRock, D. L., A. F. Johnson, S. Wilde, J. S. Sands, M. Monteiro *et al.*, 2022 Group A Streptococcus induces GSDMA-dependent pyroptosis in keratinocytes. Nature 605: 527–531.

Logger, J. G. M., E. M. G. J. de Jong, R. J. B. Driessen, and P. E. J. van Erp, 2020 Evaluation of a simple image-based tool to quantify facial erythema in rosacea during treatment. Skin Research and Technology 26: 804–812.

Mills, K. B., P. Roy, J. M. Kwiecinski, P. D. Fey, and A. R. Horswill Staphylococcal Corneocyte Adhesion: Assay Optimization and Roles of Aap and SasG Adhesins in the Establishment of Healthy Skin Colonization. Microbiol Spectr 10: e02469-22.

Missiakas, D., and V. Winstel, 2021 Selective Host Cell Death by Staphylococcus aureus: A Strategy for Bacterial Persistence. Frontiers in Immunology 11:.

Molecular Microbiology | Microbiology Journal | Wiley Online Library.

Nickerson, N., J. Ip, D. T. Passos, and M. J. McGavin, 2010 Comparison of Staphopain A (ScpA) and B (SspB) precursor activation mechanisms reveals unique secretion kinetics of proSspB (Staphopain B), and a different interaction with its cognate Staphostatin, SspC. Molecular Microbiology 75: 161–177.

Orning, P., E. Lien, and K. A. Fitzgerald, 2019 Gasdermins and their role in immunity and inflammation. J Exp Med 216: 2453–2465.

Raharja, A., S. K. Mahil, and J. N. Barker, 2021 Psoriasis: a brief overview. Clin Med (Lond) 21: 170–173.

Sabat, A. J., M. Wouthuyzen-Bakker, A. Rondags, L. Hughes, V. Akkerboom *et al.*, 2022 Case Report: Necrotizing fasciitis caused by Staphylococcus aureus positive for a new sequence variant of exfoliative toxin E. Frontiers in Genetics 13:.

Sawant, K. V., K. M. Poluri, A. K. Dutta, K. M. Sepuru, A. Troshkina *et al.*, 2016 Chemokine CXCL1 mediated neutrophil recruitment: Role of glycosaminoglycan interactions. Sci Rep 6: 33123.

Stelzner, K., A. Boyny, T. Hertlein, A. Sroka, A. Moldovan *et al.*, 2021 Intracellular Staphylococcus aureus employs the cysteine protease staphopain A to induce host cell death in epithelial cells. PLoS Pathog 17: e1009874.

Takatsu, K., 2011 Interleukin-5 and IL-5 receptor in health and diseases. Proc Jpn Acad Ser B Phys Biol Sci 87: 463–485.

Taylor, T. A., and C. G. Unakal, 2024 Staphylococcus aureus Infection, in *StatPearls*, StatPearls Publishing, Treasure Island (FL).

Tong, S. Y. C., J. S. Davis, E. Eichenberger, T. L. Holland, and V. G. Fowler, 2015 Staphylococcus aureus Infections: Epidemiology, Pathophysiology, Clinical Manifestations, and Management. Clinical Microbiology Reviews 28: 603–661.

Totté, J. E. E., W. T. van der Feltz, L. G. M. Bode, A. van Belkum, E. J. van Zuuren *et al.*, 2016 A systematic review and meta-analysis on Staphylococcus aureus carriage in psoriasis, acne and rosacea. Eur J Clin Microbiol Infect Dis 35: 1069–1077.

Towne, J. E., and J. E. Sims, 2012 IL-36 in psoriasis. Curr Opin Pharmacol 12: 486–490.

Watkins, R. R., M. Z. David, and R. A. Salata, 2012 Current concepts on the virulence mechanisms of meticillin-resistant Staphylococcus aureus. J Med Microbiol 61: 1179–1193.

Wertheim, H. F., D. C. Melles, M. C. Vos, W. van Leeuwen, A. van Belkum *et al.*, 2005 The role of nasal carriage in Staphylococcus aureus infections. The Lancet Infectious Diseases 5: 751–762.

Wilde, S., A. Dash, A. Johnson, K. Mackey, C. Y. M. Okumura *et al.*, 2023 Detoxification of reactive oxygen species by the hyaluronic acid capsule of group A Streptococcus. Infection and Immunity 0: e00258-23.

Yoshida, K., M. Takahashi, T. Ohtomo, Y. Usui, and S. Narikawa, 1979 Factors causing the clumping reaction of streptococcal strains with human plasma. J Infect Dis 139: 242–245.